Prevalence of FOXP3$^+$ Regulatory T Cells Increases During the Progression of Pancreatic Ductal Adenocarcinoma and Its Premalignant Lesions

Nobuyoshi Hiraoka,[1] Kaoru Onozato,[1] Tomoo Kosuge,[2] and Setsuo Hirohashi[1]

Abstract

Purpose: Antitumor immune response changes drastically during the progression of cancers. Established cancers often escape from the host immune system, although specific immune surveillance operates in the early stages of tumorigenesis in murine models. $CD4^+CD25^+$ regulatory T cells (T_R) play a central role in self-tolerance and suppress effective antitumor immune responses. The aim of this study was to investigate the clinical significance and roles of T_R in the progression and multistep carcinogenesis of pancreatic ductal adenocarcinoma.

Experimental Design: We raised anti-FOXP3 antibodies and used them in immunohistochemical studies of the prevalence of $FOXP3^+CD4^+CD25^+$ T_R in the $CD4^+$ T cells, which infiltrated in tissue and draining lymph nodes of 198 pancreatic ductal adenocarcinomas, their premalignant lesions (84 lesions of pancreatic intraepithelial neoplasias and 51 intraductal papillary-mucinous neoplasms), and 15 nonneoplastic pancreatic lesions.

Results: The prevalence of T_R was significantly increased in the ductal adenocarcinomas compared with that in the stroma of nonneoplastic inflammation ($P < 0.0001$). The increased prevalence of T_R was significantly correlated with certain clinicopathologic factors. A better prognosis was observed in patients with a low prevalence of T_R, and this was independent of other survival factors ($P < 0.0001$). Infiltration of intraepithelial $CD8^+TIA\text{-}1^+$ cytotoxic T cells in pancreatic ducts was marked in low-grade premalignant lesions but diminished during the progression of both pancreatic intraepithelial neoplasias and intraductal papillary-mucinous neoplasms. Conversely, the prevalence of T_R increased significantly during the progression of premalignant lesions.

Conclusions: T_R play a role in controlling the immune response against pancreatic ductal carcinoma from the premalignant stage to established cancer. In pancreatic ductal carcinoma, a high prevalence of T_R seems to be a marker of poor prognosis.

Tumors express many neoantigens originated from the vast number of genetic and epigenetic changes associated with carcinogenesis. Patients with cancer can develop tumor-specific immune responses, although established cancer usually progresses despite the antitumor immune response. It has been suggested that progressive tumors may develop immune escape strategies that include mechanisms to resist immune surveillance and induce immunotolerance. Such mechanisms might include direct deletion of immune effector cells by expression of death-inducing ligands, suppression of tumor-reactive T cells by regulatory T cells (T_R), and tolerization of host T cells by cross-presentation of tumor-derived antigens (1, 2). In contrast to established cancers, there is strong evidence from murine models that specific immune surveillance systems operate at early stages of tumorigenesis, that is, host immune system inhibits the development of tumors (3). It remains to be elucidated how and when effective immune surveillance is overcome during tumor progression. We need effective immunotherapies for aggressive cancers, such as pancreatic cancer, because they are resistant to current treatment. Thus, it is important to understand the mechanisms by which the host immune response changes and the tumor escapes from host immune surveillance during tumorigenesis and tumor progression.

Pancreatic cancer is the fourth and fifth leading cause of cancer-related death in the United States and Japan, respectively (4, 5). Because of its aggressive growth and early metastatic dissemination, the overall 5-year survival rate for pancreatic cancer is <5%, and only 20% of patients can be treated by surgery at the time of diagnosis (6–9). Many morphologic and genetic studies (10–13) strongly suggested that pancreatic intraepithelial neoplasias (PanIN) are the most major premalignant lesions for ductal adenocarcinoma. The next major is

Authors' Affiliations: [1]Pathology Division, National Cancer Center Research Institute and [2]Division of Hepatobiliary and Pancreatic Surgery, National Cancer Center Central Hospital, Tokyo, Japan

Received 2/17/06; revised 5/13/06; accepted 6/7/06.

Grant support: Ministry of Health, Labor, and Welfare of Japan Grant-in-Aid for Third Term Comprehensive 10-year Strategy for Cancer Control (S. Hirohashi) and Ministry of Education, Culture, Sports, Science and Technology of Japan Grant-in-Aid for Scientific Research (N. Hiraoka).

The costs of publication of this article were defrayed in part by the payment of page charges. This article must therefore be hereby marked *advertisement* in accordance with 18 U.S.C. Section 1734 solely to indicate this fact.

Requests for reprints: Nobuyoshi Hiraoka, Pathology Division, National Cancer Center Research Insitute, 5-1-1 Tsukiji, Chuo-ku, Tokyo 104-0045, Japan. Phone: 81-3-3542-2511; Fax: 81-3-3248-2463; E-mail: nhiraoka@gan2.res.ncc.go.jp.

doi:10.1158/1078-0432.CCR-06-0369

Table 1. Patient and tumor characteristics

A. Ductal adenocarcinoma	
Total cases	198
Age (y)	
Mean (±SD)	62 ± 10
Median (range)	63 (33-83)
Gender	
Male	114
Female	84
Tumor size (mm)	
Mean (±SD)	39.5 ± 16.8
Median (range)	35 (110-10)
Pathologic tumor status*	
pT_1	12
pT_2	26
pT_3	101
pT_4	59
Pathologic node status*	
pN_0	34
pN_{1a}	36
pN_{1b}	128
Pathologic metastasis status*	
pM_0	132
pM_1	66
Stage*	
I	16
II	10
III	74
IVA	32
IVB	66
Tumor grade†	
1	24
2	140
3	24
Other histologic type	10
B. IPMN	
Total cases	51
Age (y)	
Mean (±SD)	65 ± 8
Median (range)	66 (41-78)

Table 1. Patient and tumor characteristics (Cont'd)

B. IPMN	
Gender	
Male	31
Female	20
Tumor grade†	
IPMA	18 (intraductal hyperplasia 7 + IPMA with mild atypia 11)‡
IPMN with moderate dysplasia	7 (IPMA with moderate atypia 7)‡
IPMC, noninvasive	9 (IPMC, noninvasive 9)‡
IPMC, invasive	17 (IPMC, minimally invasive 9 + invasive carcinoma derived from intraductal tumor 8)‡
C. Nonneoplastic pancreatic lesion	
Total cases	15
Age (y)	
Mean (±SD)	60.3 ± 8.8
Median (range)	59 (48-76)
Gender	
Male	14
Female	1
Histopathologic diagnosis	
Pseudocyst	7
Chronic pancreatitis, nonspecific	4
Abscess	2
Aneurysm of splenic artery	2

*Classified according to International Union Against Cancer tumor-node-metastasis classification.
†Classified according to WHO classification.
‡Classified according to the classification of pancreatic carcinoma of Japan Pancreas Society.

intraductal papillary-mucinous neoplasms (IPMN). PanINs are microscopic lesions that are classified into PanIN-1A, PanIN-1B, PanIN-2, and PanIN-3. PanIN-1A is the earliest and mildest change and PanIN-3 is the highest grade lesion, corresponding to carcinoma *in situ*. IPMNs are a well-characterized clinical and pathologic entity featuring intraductal proliferation of neoplastic mucinous cells, which usually form papillae and lead to cystic dilation of the pancreatic ducts, forming clinically and macroscopically detectable masses (10, 12, 13). Similar to the well-defined adenoma-carcinoma sequence in colorectal cancer and PanINs (14), IPMNs seem to progress from intraductal papillary-mucinous adenoma (IPMA) to IPMN with moderate dysplasia (or borderline IPMN) and then to intraductal papillary-mucinous carcinoma (IPMC) without invasion and eventually to invasive adenocarcinoma.

Recently, thymic-derived $CD4^+CD25^+$ T_R seem to be a functionally unique population of T cells. T_R maintain immune homeostasis in immunotolerance and the control of autoimmunity. It is also related to transplantation immunity and tumor immunity. T_R can inhibit immune responses mediated by $CD4^+CD25^-$ and $CD8^+$ T cells *in vitro* by a contact-dependent and cytokine-independent mechanism (15–18), although more recent reports suggest that the immune suppression mechanisms of T_R *in vivo* are more complex (19–21). Now, FOXP3 (murine counterpart is Foxp3), a member of the forkhead or winged helix family of transcription factors, is thought to be the most reliable marker for T_R. *Foxp3/FOXP3* is disrupted in scurfy mouse (22) and in the human disorder of immune dysregulation, polyendocrinopathy, enteropathy, and X-linked inheritance (IPEX), both of which are characterized by lack of $CD4^+CD25^+$ T_R (23). *Foxp3* gene knockout mice show the same phenotype as scurfy mutant mice. The expression of Foxp3 is highly restricted to T_R and is associated with T_R activity and phenotype (24, 25). In fact, gene transfer of Foxp3 converts naive $CD4^+CD25^-$ T cells to functional T_R (26). Therefore, Foxp3/FOXP3 seems to be critical for the development and function of T_R in mouse and human (20, 21, 27). Furthermore, recent reports showed $CD4^+CD25^+Foxp3^-$ T cells did not show T_R function, although both $CD4^+CD25^+Foxp3^+$ and $CD4^+CD25^-Foxp3^+$ T cells had T_R function (28). Therefore, Foxp3/FOXP3 should be used as a marker to evaluate real T_R.

In murine models, it has been described that T_R inhibit the antitumor immune response (19, 29–31). The involvement

of $CD4^+CD25^+$ T_R in human cancer has been observed in peripheral blood and tumor tissues from patients with several types of cancer (32–35). In most of the previous studies, T_R cells were collected from fresh tissue, ascites, or blood and analyzed as $CD4^+CD25^+$ cells by flow cytometry. Until the T_R are evaluated using FOXP3-specific antibodies, it has been difficult to analyze the detailed distribution of T_R in tumors and surrounding tissues or to examine the prevalence of T_R in small premalignant lesions detected only by microscopy.

In this study, we established monoclonal antibodies that are specific for human FOXP3 protein and that can be used in immunohistochemistry of paraffin-embedded tissue sections. Using the monoclonal antibodies, we evaluated the prevalence of T_R infiltration in tumor tissues, nonneoplastic inflammatory tissues, and draining lymph nodes in 198 patients with pancreatic ductal adenocarcinoma and 15 patients with nonneoplastic pancreatic lesions. We also investigated the relationship between the prevalence of T_R and clinicopathologic findings. Furthermore, we investigated the relationship between

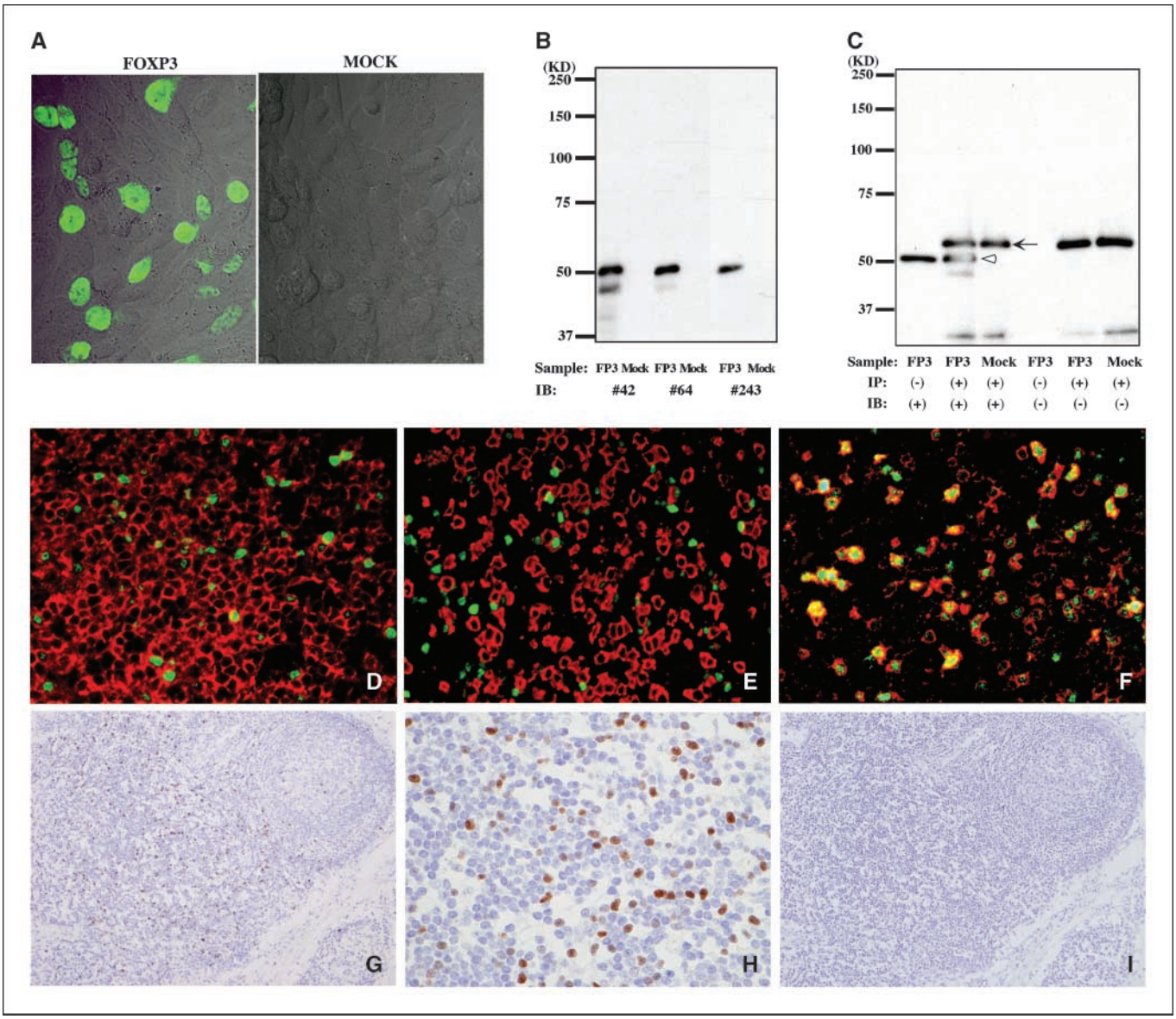

Fig. 1. *A* to *C,* establishment of monoclonal antibodies specifically reactive with FOXP3. *A,* CHO cells were transfected with pcDNA3.1-FOXP3 (*FOXP3*) or pcDNA3.1 (*MOCK*). Forty-eight hours after the transfection, cells were immunostained with anti-FOXP3 antibody 42 followed by biotin-conjugated goat-anti-mouse IgG, avidin-biotin complex method reagents, and then FITC-conjugated avidin. *B* and *C,* cell lysates from CHO cells transfected with pcDNA3.1-FOXP3 (*FP3*) or with pcDNA3.1 (*Mock*) were separated by 10% SDS-PAGE and immunoblotted with anti-FOXP3 antibodies 42, 64, and 243 (*B*). The diluted cell lysates were immunoprecipitated with anti-FOXP3 antibody 42 and immunoblotted with anti-FOXP3 antibody 64 (*C*). Arrowhead, FOXP3 protein; arrow, anti-FOXP3 antibody. *D* to *I,* FOXP3 is preferentially expressed in $CD3^+CD4^+CD25^+$ T_R located mainly in the paracortical area of lymph nodes. Anti-FOXP3 antibody 42 was used in the experiments. *D* to *F,* double immunofluorescent staining of a lymph node on a formalin-fixed paraffin-embedded section. FITC (*green*) shows positive nuclear staining of FOXP3 and Texas Red (*red*) shows positive membrane staining of CD4 (*D*), CD8 (*E*), and CD25 (*F*). *G* to *I,* immunohistochemical detection of $FOXP3^+$ cells. Peripheral lymph node was immunostained with FOXP3 and counternuclear stained with hematoxylin. $FOXP3^+$ cells were distributed mainly in the paracortical area, although sometimes small numbers of $FOXP3^+$ cells were found in follicles, even in the follicular center. Different parts of the paracortical area in the same lymph node usually showed different numbers of $FOXP3^+$ cells. Low (*G*) and high (*H*) magnification. Isotype-matched staining was in (*I*).

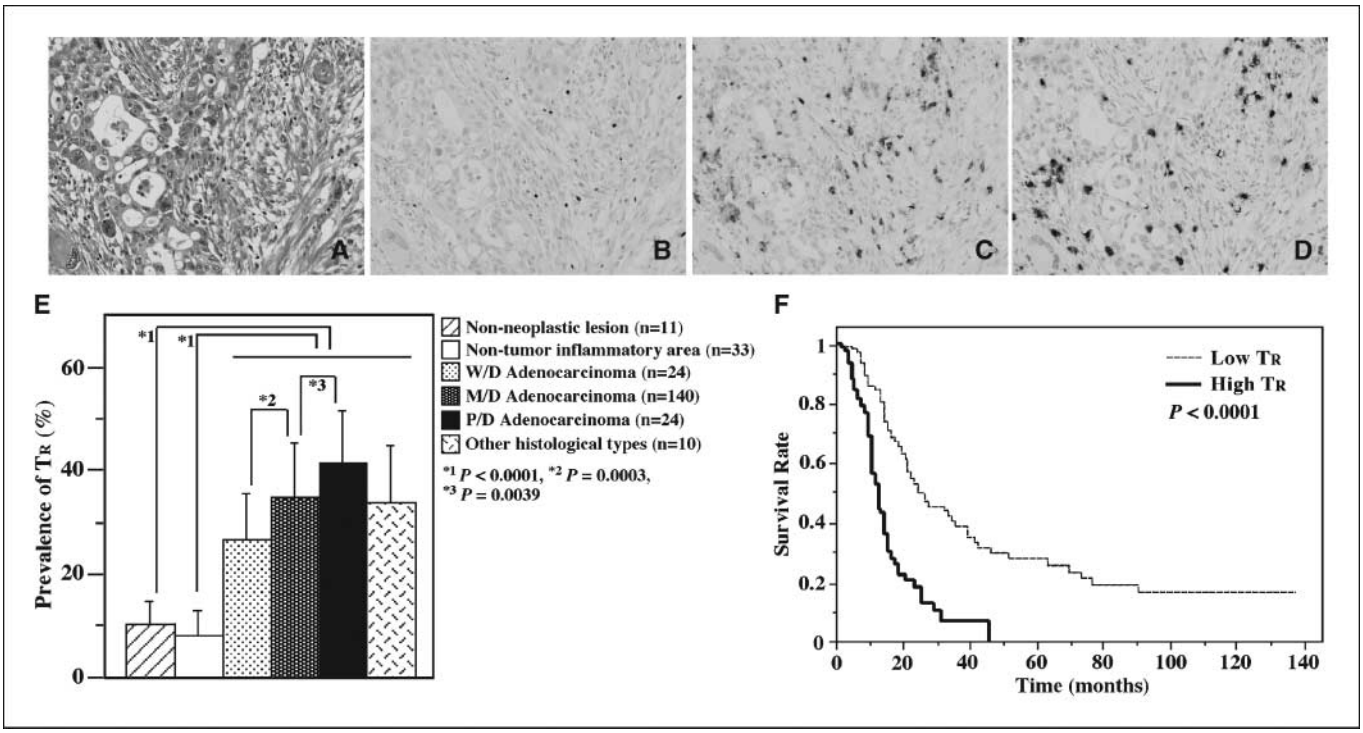

Fig. 2. Increased population of FOXP3$^+$ T_R in tumor stroma of pancreatic ductal adenocarcinoma. *A* to *D,* representative features of invasive ductal adenocarcinoma of the pancreas, moderately differentiated tubular adenocarcinoma, in HE staining (*A*) and immunostaining with FOXP3 (*B*), CD4 (*C*), and CD8 (*D*). *E,* prevalence of T_R in stroma of pancreatic ductal adenocarcinoma and nonneoplastic inflammatory lesion. Adenocarcinomas were divided into four categories: well-differentiated tubular adenocarcinoma (*W/D*; tumor grade 1), moderately differentiated tubular adenocarcinoma (*M/D*; tumor grade 2), poorly differentiated tubular adenocarcinoma (*P/D*; tumor grade 3), and other histologic types containing mucinous carcinoma and adenosquamous cell carcinoma. We also evaluated the prevalence of T_R in noncancer inflammatory stroma from patients with nonneoplastic pancreatic lesions (nonneoplastic inflammation area) and pancreatic adenocarcinoma (nontumor inflammatory area). *F,* Kaplan-Meier survival curves of 198 patients. The prognosis was significantly worse in the high prevalence of T_R group (*solid line*; $n = 94$) compared with the low prevalence of T_R group (*dotted line*; $n = 104$; $P < 0.0001$, log-rank test).

the prevalence of T_R and multistep carcinogenesis by analyzing 84 lesions of PanINs and 51 cases of IPMNs, in addition to analysis of intraepithelial lymphocytes infiltrated in their intraductal premalignant lesions. We provide evidence that the prevalence of T_R increases during the progression of established cancers as well as of their premalignant lesions. Furthermore, the prevalence of T_R was significantly correlated with patient survival, independent of several prognostic factors.

Materials and Methods

Patients and samples. This study was approved by the Ethics Committee of the National Cancer Center (Tokyo, Japan). Clinical and pathologic data and the specimens used for immunohistochemical analysis were obtained through a detailed retrospective review of the medical records of all 198 patients with pancreatic ductal adenocarcinoma, 51 patients with IPMNs, and 15 patients with nonneoplastic pancreatic lesions who had undergone initial surgical resection between 1990 and 2002 at the National Cancer Center Hospital (Tokyo, Japan). All the patients had not received any prior therapy. All patients with pancreatic ductal adenocarcinoma and with IPMNs received standard therapy appropriate for their clinical stages. Along with tumor extension, lymphadenectomy was done at the hepatoduodenal ligament and around the abdominal aorta. Tumors were classified according to the WHO classification (13, 36), the International Union Against Cancer tumor-node-metastasis classification (37), and the classification of pancreatic carcinoma of the Japan Pancreas Society (38). All patients had complete medical records and had been followed by the tumor registries for survival and outcome. The latest survival data were collected on April 26, 2005. The mean follow-up was 20 months (range, 2-137 months) for patients with pancreatic ductal adenocarcinoma and 45 months (range, 2-142 months) for patients with intraductal papillary-mucinous neoplasia. The clinicopathologic features of the patients are summarized in Table 1.

Establishment of monoclonal anti-human FOXP3 antibodies. The total coding sequence of human FOXP3 amplified by PCR with specific primers (5′-ATgCCCAACCCCAggCCT-3′ and 5′-ggggCCAggTgTAgggTT-3′) was subcloned into the pBAD/Thio-TOPO vector (Invitrogen, Carlsbad, CA). After transformation of *Escherichia coli* TOP10 with this plasmid vector, the expression of FOXP3-HP-thioredoxin fusion protein was induced with arabinose and the bacterial cells were lysed with a lysis buffer [100 mmol/L NaH_2PO_4, 10 mmol/L Tris/Cl (pH 8.0), 8 mol/L urea]. To purify the FOXP3 fusion protein, the lysate was separated by 7.5% SDS-PAGE followed by copper staining with 0.3 mol/L $CuCl_2$ solution. The 60-kDa-sized single band representing FOXP3-HP-thioredoxin fusion protein was cut from the polyacrylamide gel and the FOXP3 fusion protein was extracted with a Centrilutor (Millipore, Bedford, MA). The gel extract was concentrated with a Centriprep (Millipore) and dialysed against PBS (pH 7.4). Six-week-old female BALB/c mice (Clea Japan, Inc., Tokyo, Japan) were immunized s.c. with 100 μg of purified FOXP3 fusion protein mixed with complete Freund's adjuvant per mouse. The second to fourth immunizations were done with 50 μg of the purified FOXP3 fusion protein mixed with incomplete Freund's adjuvant at 2-week intervals. After the last injection, immune splenic lymphocytes were fused with SP-2 myeloma cells by using polyethylene glycol (mixture of MW 3,350 and MW 6,000 at 3:1) according to a method described previously (39). Primary screening of the supernatants of hybridomas was done with formalin-fixed paraffin-embedded sections of lymph nodes by immunohistochemistry described below. The supernatants from several different hybridoma

clones reacted exclusively with nuclei of lymphoid cells. After repeated cloning, we selected three hybridoma clones, 42, 64, and 243, for further characterization. The immunoglobulin subclass was determined with a mouse monoclonal antibody isotyping kit (Amersham, Buckinghamshire, United Kingdom). These three clones secreted immunoglobulins of subclasses $IgG_{1\kappa}$, $IgG_{2a\kappa}$, and $IgG_{1\kappa}$, respectively.

Expression of FOXP3 protein in mammalian cells and immunocytochemistry. FOXP3 protein was expressed as described previously (40). Briefly, the full-length cDNA of human FOXP3 was subcloned into pcDNA3.1/Hyg (+) (Invitrogen) and the new vector was named pcDNA3.1-FOXP3. Chinese hamster ovary (CHO) cells (American Type Culture Collection, Rockville, MD) cultured on coverslips were transiently transfected with pcDNA3.1-FOXP3 or pcDNA3.1/Hyg by use of LipofectAMINE Plus (Invitrogen). At 48 hours after the transfection, the CHO cells were fixed with 4% paraformaldehyde containing 0.1% Triton X-100 at 4°C for 30 minutes or with chilled methanol with 10% acetone on ice for 20 minutes. The cells were stained by the avidin-biotin complex method of immunohistochemistry described below modified by using FITC-conjugated avidin instead of avidin-biotin complex method reagent and the labeling intensity was observed by confocal microscopy.

Immunoblot analysis and immunoprecipitation. CHO cells were transiently transfected with pcDNA3.1-FOXP3 or pcDNA3.1/Hyg. Forty-eight hours after transfection, both FOXP3 and mock transfectants were lysed in a lysis buffer [1% Triton X-100, a cocktail of proteinase inhibitors (Roche Diagnostics Corp., Indianapolis, IN) in PBS]. Equal amounts of protein samples were separated on 7% or 10% polyacrylamide gels and transferred to polyvinylidene difluoride membrane (Immobilon-P; Millipore). After blocking the membranes in 5% skim milk in 0.05% Tween 20 in TBS, they were incubated with anti-FOXP3 antibody followed by the incubation with peroxidase-conjugated anti-mouse Ig $F(ab')_2$ fragment (Amersham). The antigen was detected with enhanced chemiluminescence Western blotting detection reagents (Amersham) according to the manufacturer's instructions. For immunoprecipitation, equal amounts of cell lysates were precleared with protein G-Sepharose 4 Fast Flow (Amersham), then anti-FOXP3 antibody was added to the lysates, and the samples were incubated. Immune complexes were precipitated by incubating the samples with the protein G-Sepharose beads and subjected to immunoblot analysis with anti-FOXP3 antibody as described above.

Immunohistochemical analysis. Immunoperoxidase staining by the avidin-biotin-peroxidase complex method was done on formalin-fixed paraffin-embedded 4-μm-thick sections as described previously (41). To enhance the signal for CD4 (used at a dilution of 1:100; 1F6, Novocastra Laboratories Ltd., Newcastle, United Kingdom) and CD8 (used at a dilution of 1:100; 4B11, Novocastra Laboratories), we used the catalyzed signal amplification (CSA) system (DAKO, Glostrup, Denmark) according to the manufacturer's instructions. No significant staining was observed in the negative controls, which were prepared by using the same class of mouse immunoglobulin at the same concentration.

Serial sections were prepared from each paraffin block. The first section was stained with H&E and the second and third sections were subjected to immunohistochemistry to detect the CD4 and FOXP3 antigens. $CD4^+$ or $FOXP3^+$ lymphocytes were counted in the corresponding visual field. Quantitative evaluation of lymphocytes was done by analyzing at least three different high-power fields (×40 objective and ×10 eyepiece). We analyzed representative blocks and omitted pinpoint lesions because they were too small to analyze the lymphocytic infiltration at least three different high-power fields. The proportion of $FOXP3^+$ lymphocytes in the $CD4^+$ lymphocytes was calculated for each field and the averages were compared. Preliminary study revealed that absolute number of lymphocytes infiltrated was easily affected by inflammation. To reduce the effect of inflammation in evaluation of T_R, we selected the prevalence of $FOXP3^+$ T_R in $CD4^+$ T cells.

Double immunofluorescence. We did double immunofluorescent staining on formalin-fixed paraffin-embedded sections. The 4-μm-thick sections were deparaffinized and autoclaved for 10 minutes at 121°C either in 10 mmol/L citrate buffer (pH 6.0) for CD3 (used at a dilution of 1:50; UCHT1, DAKO) and CD8 or in 1 mmol/L EDTA (pH 8.0) for CD4 and CD25 (used at a dilution of 1:50; ACT-1, DAKO) followed by a wash in 0.05% Tween 20 in TBS (pH 7.6). For double staining of the sections with FOXP3 and CD3, CD4, CD8, or CD25, the last four antigens were stained by the CSA system with our modification and then FOXP3 was stained with CSAII (a biotin-free tyramide signal amplification system from DAKO). The CSA system was modified as follows. After reaction with biotin-conjugated tyramide solution, the sections were incubated with Texas Red–conjugated avidin (1:200; Vector Laboratories, Inc., Burlingame, CA) for 30 minutes at room temperature. To detach the antibodies, the sections were incubated in 100 mmol/L glycine/HCl (pH 2.2) for 2 hours at room temperature with gentle stirring. The sections were then washed in 0.05% Tween 20 in TBS and stained with FOXP3 using CSAII according to the

Table 2. Correlation between clinicopathologic findings and the prevalence of T_R

Characteristics	Ratio of T_R in $CD4^+$ T cells		*P*
	Low T_R	High T_R	
Age (y)			
≥60	43 (41.3)	39 (41.5)	
<60	61 (58.7)	55 (58.5)	0.98
Sex			
Male	62 (59.6)	52 (55.3)	
Female	42 (40.4)	42 (44.7)	0.54
Pathologic tumor status			
pT_1	7 (6.7)	5 (5.3)	
pT_2	16 (15.4)	10 (10.6)	
pT_3	56 (53.8)	45 (47.9)	
pT_4	25 (24.0)	34 (36.2)	0.29
Pathologic node status			
pN_0	22 (21.2)	12 (12.8)	
pN_{1a}	21 (20.2)	15 (16.0)	
pN_{1b}	61 (58.7)	67 (71.3)	0.16
Pathologic metastasis status			
pM_0	79 (76.0)	53 (56.4)	
pM_1	25 (24.0)	41 (43.6)	0.0035*
Stage			
I	9 (8.7)	7 (7.4)	
II	8 (7.7)	2 (2.1)	
III	45 (43.3)	29 (30.9)	
IVA	17 (16.3)	15 (16.0)	
IVB	25 (24.0)	41 (43.6)	0.029*
Tumor grade†			
1	21 (21.4)	3 (3.3)	
2	71 (72.4)	69 (76.7)	
3	6 (6.1)	18 (20.0)	0.0002*
Tumor margin status			
Negative	70 (67.3)	61 (64.9)	
Positive	34 (32.7)	33 (35.1)	0.72
Lymphatic invasion‡			
Negative	8 (7.7)	5 (5.3)	
Positive	96 (92.3)	89 (94.7)	0.5
Vascular invasion‡			
Negative	13 (12.5)	8 (8.5)	
Positive	91 (87.5)	86 (91.5)	0.36
Perineural invasion‡			
Negative	4 (3.8)	7 (7.4)	
Positive	100 (96.2)	87 (91.5)	0.27

*Significant.
†Tumors of special types of histology (adenosquamous cell carcinoma, etc.) are avoided.
‡Classified according to the classification of pancreatic carcinoma of Japan Pancreas Society.

Table 3. Hazard ratios for effect of clinicopathologic characteristics and the prevalence of T_R in $CD4^+$ T cells on overall survival

Variables	Categories	Univariate analysis		Multivariate analysis	
		Overall survival		Overall survival	
		HR (95% CI)	*P*	HR (95% CI)	*P*
Age (y)	<60 vs ≥60	1.68 (0.88-3.22)	0.12	1.30 (0.87-1.94)	0.2
Sex	Male vs female	1.03 (0.72-1.46)	0.88	1.07 (0.73-1.56)	0.74
Pathologic tumor status	$pT_1 + pT_2 + pT_3$ vs pT_4	1.16 (0.81-1.65)	0.41	1.08 (0.72-1.56)	0.71
Pathologic node status	pN_0 vs $pN_{1a} + pN_{1b}$	1.46 (1.00-2.12)	0.048*	1.97 (1.06-3.68)	0.032*
Pathologic metastasis status	pM_0 vs pM_1	2.38 (1.34-4.24)	0.0032*	1.56 (1.01-2.40)	0.045*
Tumor grade†	1 vs 2 + 3	2.19 (1.52-3.16)	<0.0001*	1.21 (0.60-2.44)	0.6
Tumor margin status	Negative vs positive	1.50 (1.05-2.14)	0.026*	1.67 (1.12-2.48)	0.012*
Prevalence of T_R in $CD4^+$ T cells	Low vs high	2.56 (1.77-3.70)	<0.0001*	2.45 (1.62-3.72)	<0.0001*

Abbreviations: HR, hazard ratio; 95% CI, 95% confidence interval.
*Significant.
†Tumors of special types of histology (adenosquamous cell carcinoma, etc.) are avoided.

manufacturer's instructions. Just after reaction of the sections with FITC-conjugated tyramide, the sections were washed and mounted with Vectashield mounting medium (Vector Laboratories). For double staining of the sections with FOXP3 and CD20 (used at a dilution of 1:200; L26, DAKO) or CD56 (used at a dilution of 1:100; NCC-Lu-243, Nihonkayaku, Tokyo, Japan), the sections were first immunostained with FOXP3 using CSAII and then stained with CD20 or CD56. Immunostained tissue sections were analyzed with a confocal microscope (LSM5 Pascal; Carl Zeiss Jena GmbH, Jena, Germany) equipped with a 15-mW Kr/Ar laser.

Statistical analysis. Values were expressed as mean ± SD. Statistical analyses were done with StatView-J 5.0 software (Abacus Concepts, Berkeley, CA). Association of the prevalence of $FOXP3^+$ cells in $CD4^+$ T cells with various clinicopathologic variables was assessed by the χ^2 test. Kruskal-Wallis nonparametric tests were used to compare the value of numbers of $CD8^+$ intraepithelial lymphocytes (IEL)/prevalence of T_R in stromal-infiltrating $CD4^+$ T cells among each grades of PanINs and IPMNs. Survival rates were calculated by the Kaplan-Meier method. Differences between survival curves were analyzed by the log-rank test. To assess the correlation between survival time and multiple clinicopathologic variables, multivariate analyses were done by the Cox proportional hazards regression model. Differences were considered significant when $P < 0.05$.

Results

Establishment of monoclonal antibodies specific for FOXP3 expressed preferentially in $CD4^+CD25^+$ T_R. We established monoclonal antibodies (42, 64, and 243) against FOXP3 protein (Materials and Methods). These antibodies stained the nuclei and sometimes the cytoplasm of CHO cells transfected with FOXP3-pcDNA3.1, which contains cDNA encoding full-length FOXP3 but did not stain mock transfectants (Fig. 1A). When we used these antibodies to do immunoblot analyses of the cell lysates obtained from both transfectants, we detected a condensed band showing the expected size of ~50 kDa in the lysate from FOXP3-transfected CHO cells. No band was recognized in lanes loaded with lysates of mock transfectants (Fig. 1B). These findings indicate that the monoclonal antibodies specifically recognize FOXP3 protein. Furthermore, the antibodies could immunoprecipitate FOXP3 protein from the diluted lysates of FOXP3-transfected CHO cells (Fig. 1C).

To examine the immunophenotype of $FOXP3^+$ cells, double immunofluorescent staining was done. All $FOXP3^+$ cells were $CD3^+$ (data not shown), almost all of them were $CD4^+$ T cells (Fig. 1D), and the majority of the $FOXP3^+$ cells were $CD25^+$ (Fig. 1F). In contrast, no expression of FOXP3 was found in either $CD20^+$ B cells or $CD56^+$ natural killer cells (data not shown). The majority of $CD8^+$ T cells also did not express FOXP3, although a few did so (Fig. 1E). These findings confirm that the majority of $FOXP3^+$ cells are $CD4^+CD25^+$ T cells, with a minor population of $FOXP3^+CD4^+CD25^-$ T cells and a few $FOXP3^+CD8^+$ T cells. $FOXP3^+$ cells were distributed mainly in the paracortical area in lymph nodes (Fig. 1G and H). There were no $FOXP3^+$ tissues or cells, except lymphoid cells in brain, liver, lung, kidney, esophagus, stomach, intestine, colon, pancreas, heart, skin, and skeletal muscle. Previous studies have shown that $FOXP3^+CD4^+CD25^+$ T cells exclusively belong to T_R (18, 20, 21, 27). These findings allowed us to conclude that the monoclonal antibodies we established can specifically detect T_R in formalin-fixed paraffin-embedded tissue sections. We used anti-FOXP3 antibody 42 in the later experiments.

Increased populations of $FOXP3^+T_R$ in $CD4^+$ T cells in tumor stroma of pancreatic ductal adenocarcinoma. Stromal-infiltrated lymphocytes both from tumor stroma and from nonneoplastic inflammatory stroma in patients with pancreatic ductal adenocarcinoma (n = 198) and nonneoplastic pancreatic lesions (n = 11) were examined for the prevalence of $FOXP3^+$ T_R. Histologically, lymphocytic infiltration was present in cancer stroma and was usually seen frequently in obvious cancer invasion, particularly in areas where cancer cells had just invaded the surrounding tissue. The prevalence of T_R in $CD4^+$ T cells was not markedly different between the central and peripheral areas of cancers. Representative immunohistochemical features are shown in Fig. 2A-D. T_R usually infiltrated into stroma and rarely into the epithelial layer of ducts, although T_R occasionally attached directly to cancer cells. Summarized data from all patients indicated that the prevalence of tumor-infiltrating T_R in $CD4^+$ T cells in pancreatic ductal adenocarcinoma (34.6 ± 10.9%) was significantly higher than that in nonneoplastic inflammatory areas from patients with pancreatic ductal adenocarcinoma (7.9 ± 4.9%; $P < 0.0001$) and in nonneoplastic pancreatic lesions (10.1 ± 4.6%; $P < 0.0001$;

Fig. 2E). The prevalence of T_R in $CD4^+$ T cells was significantly higher in less-differentiated adenocarcinoma [well-differentiated adenocarcinoma versus moderately differentiated adenocarcinoma (P = 0.0003); moderately differentiated adenocarcinoma versus poorly differentiated adenocarcinoma (P = 0.0039); Fig. 2E]. Although lymphocytic infiltration was rare in nonneoplastic and noninflammatory areas, it was sometimes marked in nonneoplastic but inflammatory areas compared with cancer stroma. Despite this finding, the prevalence of T_R in $CD4^+$ T cells was significantly increased in the stroma of adenocarcinoma compared with nonneoplastic inflammatory areas, suggesting that adenocarcinoma cells recruit T_R to themselves. Our observations also suggest that the prevalence of T_R is closely correlated with cancer progression.

Prevalence of T_R in $CD4^+$ T cells and clinicopathologic features of pancreatic ductal adenocarcinoma. We next analyzed the correlation between clinicopathologic features of pancreatic ductal adenocarcinoma and the prevalence of T_R in $CD4^+$ T cells. Patients with pancreatic cancers were divided into two groups of high T_R (n = 94) and low T_R (n = 104), representing higher and lower than average (34.6%) prevalence of T_R in $CD4^+$ T cells. High prevalence of T_R was significantly correlated with distant metastasis (P = 0.0035; Table 2), advanced tumor stage (P = 0.029), and high tumor grade (P = 0.0002) among the various clinicopathologic features tested (Table 2).

Prognostic significance of prevalence of T_R in $CD4^+$ T cells. Overall survival was analyzed in these patients. Fourteen of 198 (7%) patients survived >5 years after surgical resection, and 24 (12%) patients survived >3 years. The low-T_R group

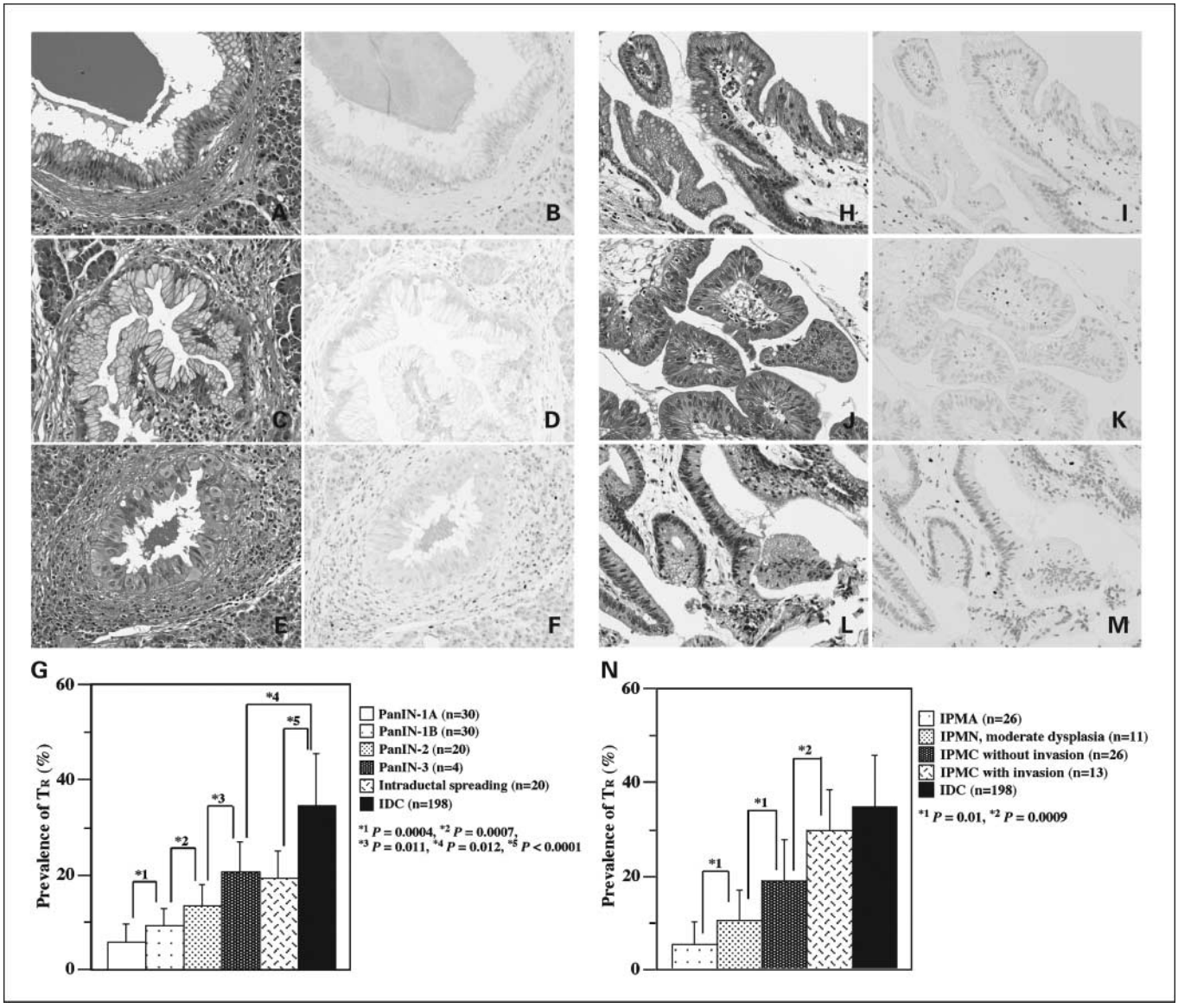

Fig. 3. Increased population of T_R in tumor stroma corresponding to the progression of PanINs and IPMNs. *A* to *F,* representative features of PanIN-1A (*A* and *B*), PanIN-1B (*C* and *D*), and intraductal spreading of adenocarcinoma (*E* and *F*) in HE staining (*A, C*, and *E*) and immunostaining with FOXP3 (*B, D*, and *F*). *G,* prevalence of T_R in stroma surrounding pancreatic ducts occupied by intraductal lesions or stroma of invasive ductal adenocarcinoma (*IDC*). Intraductal spreading: Intraductal spreading of adenocarcinoma without invasion of cancer cells surrounding the duct. *H* to *M,* representative features of IPMA (*H* and *I*), IPMN with moderate dysplasia (*J* and *K*), and IPMC without invasion (*L* and *M*) in HE staining (*H, J*, and *L*) and immunostaining with FOXP3 (*I, K*, and *M*). *N,* prevalence of T_R in stroma surrounding pancreatic ducts occupied by intraductal lesions or stroma of invasive ductal adenocarcinoma. Thin bars, SD.

showed significantly better survival rates than did the high-T_R group ($P < 0.0001$, log-rank test; Fig. 2F). Mean survival ($\pm$SD) was 26.2 ($\pm$29.4) months for the low-T_R group and 13.4 ($\pm$15.0) months for the high-T_R group. In the low-T_R group, 21 of 24 (87%) patients survived >3 years after the operation and 15 patients died within a year. In the high-T_R group, 3 of 24 (13%) patients survived >3 years after the operation and 47 patients died within a year. We found that lymph node

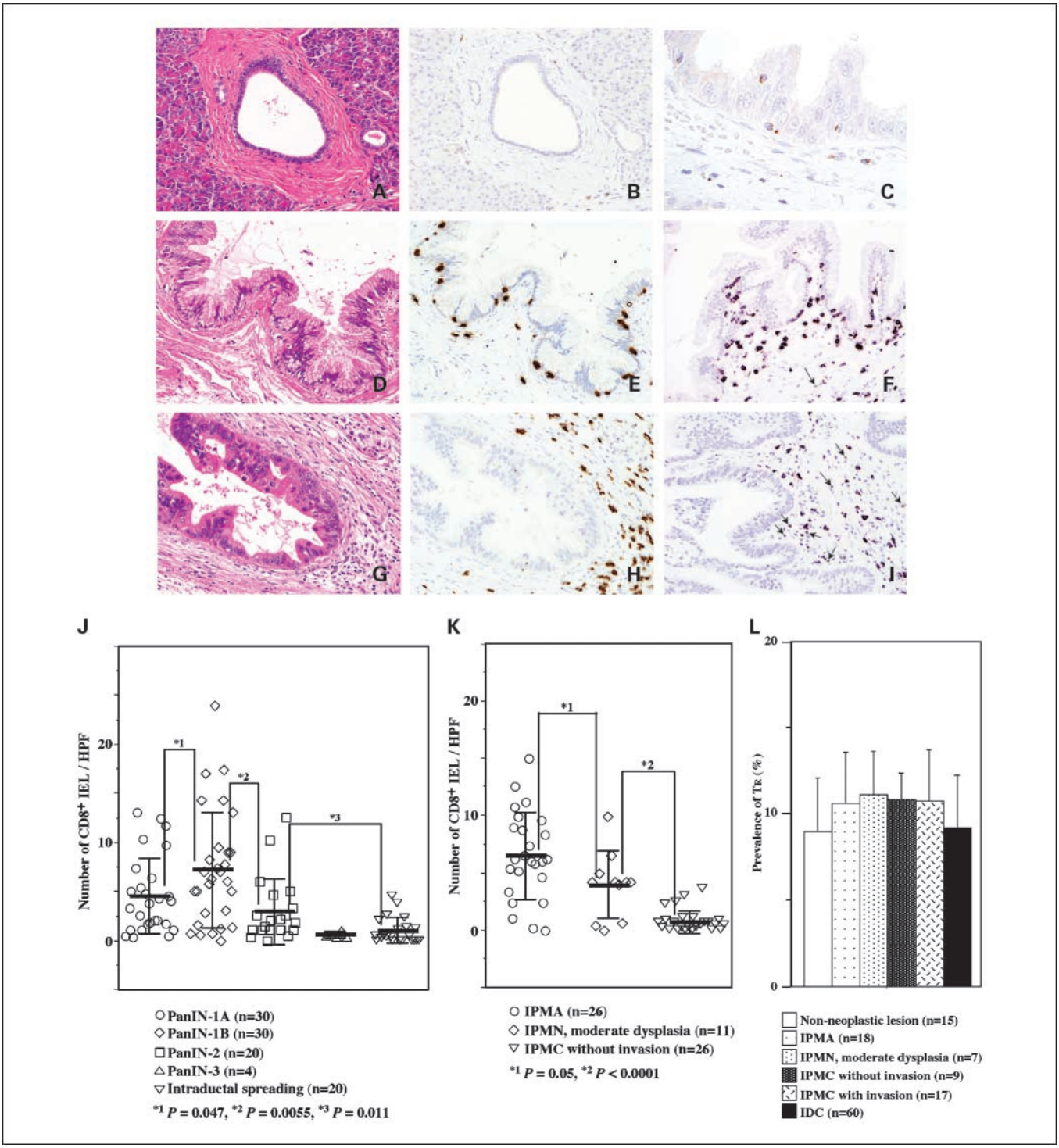

Fig. 4. Infiltration of $CD8^+$ IEL was marked in low-grade premalignant lesions, diminished in borderline lesions, and eventually disappeared in carcinoma *in situ*. *A* to *G*, representative features of normal duct (*A* and *B*), PanIN-1B (*C*, *D*, and *G*), and intraductal spreading of adenocarcinoma (*E* and *F*) in HE staining (*A*, *C*, and *E*) and immunostaining with CD8 (*B*, *D*, and *F*). The majority of the $CD8^+$ IEL expressTIA-1 (*G*). *H* and *I*, representative features of IPMA (*H*) and IPMC (*I*) in double immunostaining with FOXP3 (*brown*) and CD8 (*purple*). In IPMA (*H*), there were many $CD8^+$ IEL, stromal infiltrating $CD8^+$ Tcells, and few $FOXP3^+$ cells (*arrow*) around ducts. Although there was no $CD8^+$ IEL, we observed stromal infiltrating $CD8^+$ Tcells and several $FOXP3^+$ cells (*arrows*) around ducts in IPMC without invasion (*I*). No $FOXP3^+$ IEL was found. *J* and *K*, average number of $CD8^+$ IEL in intraductal lesions of PanINs (*J*) or IPMNs (*K*). Thick bar and thin bars are average and $\pm$SD, respectively. Intraductal spreading: Intraductal spreading of adenocarcinoma without invasion of cancer cells surrounding the duct. *L*, prevalence of T_R in the draining lymph nodes was not significantly changed among patients with nonneoplastic pancreatic lesions, patients with IPMNs, and patients with invasive ductal adenocarcinoma. Thin bars are $\pm$SD.

metastasis, distant metastasis, and tumor margins were independent factors for patient survival in our retrospective study using multivariate analysis for the standard clinicopathologic factors. In multivariate Cox proportional hazard analysis for clinicopathologic variables and prevalence of T_R in $CD4^+$ T cells, the hazard ratio for poor prognosis was 2.45 for patients in the high-T_R group compared with patients in the low-T_R group ($P < 0.0001$; Table 3).

Increased populations of T_R in $CD4^+$ T cells in tumor stroma correspond to progression during multistep carcinogenesis both in PanINs to invasive ductal adenocarcinoma and in IPMNs. The prevalence of T_R in $CD4^+$ T cells in the ducts of PanINs and IPMNs was analyzed during tumorigenesis and progression of pancreatic adenocarcinoma. Thirty lesions of PanIN-1A (Fig. 3A and B), 30 lesions of PanIN-1B (Fig. 3C and D), 20 lesions of PanIN-2, and 4 lesions of PanIN-3 were randomly selected for this examination. We carefully defined PanIN-3 lesions to avoid possible contamination by intraductal spreading of invasive ductal adenocarcinoma. For this definition, we cut all the pancreas to make sections and carried out histopathologic examination and then defined PanIN-3 as an apparently solitary lesion that was not connected to invasive ductal adenocarcinoma. All these lesions were distant from invasive cancer. However, it is sometimes difficult to differentiate PanIN-3 from intraductal spreading of invasive ductal adenocarcinoma when the intraductal lesion is located next to the invasive ductal adenocarcinoma with obscure connection or without an abrupt transition from markedly atypical to normal-appearing epithelium. For such lesions in our series, we established another category "intraductal spreading of ductal adenocarcinoma without invasive cancer cells surrounding the duct" (Fig. 3E and F) and additionally examined the prevalence of T_R in such lesions. We found a significant increase of the prevalence of T_R in $CD4^+$ T cells during the progression from low-grade PanIN to invasive ductal carcinoma [PanIN-1A versus PanIN-1B ($P = 0.0004$), PanIN-1B versus PanIN-2 ($P = 0.0007$), PanIN-2 versus PanIN-3 ($P = 0.011$), PanIN-2 versus intraductal spreading ($P = 0.0005$), PanIN-3 versus invasive ductal adenocarcinoma ($P = 0.012$), and intraductal spreading versus invasive ductal adenocarcinoma ($P < 0.0001$); Fig. 3G]. The prevalence was similar between PanIN-3 and intraductal spreading of adenocarcinoma ($P = 0.68$).

IPMNs usually contain lesions with various degrees of cellular and structural atypism and are diagnosed as the highest grade of the lesions. To examine the relationship between the prevalence of T_R and each grade of IPMN lesion during tumor progression, we classified IPMNs from 51 cases into 27 lesions of IPMA (Fig. 3H and I), 10 lesions of borderline (Fig. 3J and K), 19 lesions of IPMC without invasion (Fig. 3L and M), and 13 lesions of IPMC with invasion according to the WHO classification. Then, we evaluated $FOXP3^+$ and $CD4^+$ T cells in each grade of IPMN lesion. As shown in Fig. 3N, the prevalence of T_R in $CD4^+$ T cells increased significantly in a stepwise manner and parallel with the progression of IPMNs [IPMA versus IPMN, moderate dysplasia ($P = 0.01$); IPMN, moderate dysplasia versus IPMC without invasion ($P = 0.01$)]. There was a particularly marked increase in prevalence when IPMC began to invade ($P = 0.0009$). These findings suggest that the prevalence of T_R is closely correlated with the progression of premalignant lesions, both PanINs and IPMNs. Clinical follow-up revealed that tumors recurred in 4 of 17 patients with IPMC with invasion, of whom 3 died 17, 21, and 23 months after the operation. No significant difference in the prevalence of T_R was noted between cases with recurrence and no recurrence.

Host immune response was marked in low-grade premalignant lesions but diminished and eventually disappeared during carcinogenesis. To estimate the extent of host immune response to these intraductal lesions, we did immunohistochemistry to detect infiltrating lymphocytes. We found that $CD8^+$ T cells infiltrated as IEL in premalignant lesions as well as stromal-infiltrating lymphocytes around the ducts (Fig. 4C and D). In noninflammatory and nonneoplastic ducts, no IELs were apparent (Fig. 4A and B). In both inflammatory and premalignant lesions, the majority of IEL in small- and large-sized pancreatic ducts consisted of $CD3^+CD8^+$ T cells with some $CD4^+$ T cells, a few $CD56^+$ natural killer cells, and no $CD20^+$ B cells. Interestingly, there was marked infiltration of $CD8^+$ IEL in PanIN-1A and PanIN-1B, significantly decreased numbers in PanIN-2, and few IEL in PanIN-3 or intraductal spreading of adenocarcinoma [PanIN-1B versus PanIN-2 ($P = 0.0055$); PanIN-2 versus intraductal spreading ($P = 0.011$); Fig. 4A-F and J]. Most of these IELs showed cytoplasmic granular expression of TIA-1 (T-cell intracellular antigen-1), indicating that they were cytotoxic T cells (Fig. 4G).

In IPMNs, there was a marked infiltration of IEL in low-grade IPMNs, but infiltration was never or seldom observed in IPMC [IPMA versus IPMN, moderate dysplasia ($P = 0.05$); IPMN, moderate dysplasia versus IPMC without invasion ($P < 0.0001$); Fig. 4K]. These findings suggest that a host immune response was present in low-grade premalignant lesions, diminished during the progression of the premalignant lesions, and then almost disappeared in noninvasive adenocarcinomas. It was very rare that $FOXP3^+$ T_R infiltrated as IEL in pancreatic ducts and we did not observe $CD8^+$ IEL bound to T_R IEL in any stages of lesions (Fig. 4H and I). When we compared the ratio of $CD8^+$ IEL counts with the prevalence of $FOXP3^+$ T_R infiltrated in stroma around the ducts, the ratio showed the same tendencies to the changes of amounts in $CD8^+$ IEL infiltrated during the progression of PanINs ($P < 0.0001$, Kruskal-Wallis test) and IPMNs ($P < 0.0001$, Kruskal-Wallis test).

Prevalence of T_R in $CD4^+$ T cells in draining lymph nodes was not significantly different among nonneoplastic lesions, premalignant lesions, and invasive adenocarcinoma of pancreas. We examined the prevalence of T_R in $CD4^+$ T cells in the draining lymph nodes of the pancreas of 60 patients with invasive ductal carcinoma, 15 patients with nonneoplastic pancreatic lesions, and 51 patients with IPMNs. Patients with IPMNs were classified according to the highest grade of the lesion in the IPMNs. No significant difference in the prevalence of T_R in $CD4^+$ T cells was found among lymph nodes from patients with ductal adenocarcinoma, IPMNs, and nonneoplastic pancreatic lesions (Fig. 4L).

Discussion

In this study, we found that there is a relationship between T_R and pancreatic carcinogenesis. To detect T_R in microscopic premalignant lesions, we raised new monoclonal antibodies to FOXP3. The prevalence of $FOXP3^+CD4^+$ T_R in tissue-infiltrating $CD4^+$ T cells was evaluated in pancreatic ductal adenocarcinomas, their premalignant lesions, and nonneoplastic inflammatory

lesions. The prevalence of T_R was significantly increased in the stroma of pancreatic invasive ductal carcinomas compared with that in the stroma of nonneoplastic inflammation of the pancreas in patients with pancreatic ductal adenocarcinoma and nonneoplastic pancreatic lesions. The prevalence of T_R was significantly correlated with clinicopathologic factors and patient prognosis. Furthermore, the prevalence of T_R increased during the progression of the invasive cancers as well as of the premalignant lesions of pancreatic ductal carcinoma, PanINs, and IPMNs. It was inversely correlated with the numbers of cytotoxic $CD8^+$ T cells infiltrated as IEL in the pancreatic ducts. Thus, we provided the first evidence that cytotoxic T cells and T_R infiltrate during multistep pancreatic carcinogenesis.

Naturally arising $CD4^+CD25^+$ T_R characteristically express CD25, CTL-associated antigen 4 (CTLA-4), glucocorticoid-induced tumor necrosis factor receptor family–related gene (GITR), surface transforming growth factor-β (TGF-β), and FOXP3. CD25 is a critical molecule for proliferation and survival of $CD4^+CD25^+$ T_R (20). However, CD25 is not a suitable marker to define T_R because activated T cells generally express CD25. Compelling studies have revealed that CTLA-4 and TGF-β play roles in the suppressive activity of $CD4^+CD25^+$ T_R against $CD4^+$ or $CD8^+$ T cells, although they are not expressed exclusively in T_R. Experiments with *Foxp3*-over-expressing transgenic or *Foxp3* gene-depleted mice and other studies have shown that *Foxp3*/*FOXP3* is a master control gene for the development and function of natural $CD4^+CD25^+$ T_R (20, 21, 27, 28). Thus, Foxp3/FOXP3 is thought to be a suitable single marker for detecting $CD4^+CD25^+$ T_R. Our newly established antibodies reacted specifically with FOXP3 protein. Most $FOXP3^+$ cells were $CD4^+CD25^+$ T cells and the remaining minor population of $FOXP3^+$ cells was $CD4^+CD25^-$ T cells. Zelenay et al. (42) reported that $FOXP3^+CD4^+CD25^-$ T cells convert to $CD25^+$ after homeostatic expansion and/or activation in the murine model and they concluded that $FOXP3^+CD4^+CD25^-$ T cells constitute a peripheral reservoir of committed regulatory cells. These findings indicate that our antibodies detected the entire population of regulatory $CD4^+$ T cells committed to $FOXP3^+CD4^+CD25^+$ T_R. The prevalence of T_R in our study seemed to be higher than in previous studies (33). We found that the intensity of staining for T_R usually differed between cancer stroma and inflammatory areas, and our values for prevalence are limited to cancer stroma alone, with little dilution of the values by contaminating noncancer stroma.

In murine models, T_R inhibit the antitumor immune response mediated by $CD4^+CD25^-$ T cells and $CD8^+$ cytotoxic T cells (19, 29–31). In humans, the prevalence of $CD4^+CD25^+$ T cells in $CD4^+$ T cells has been shown to increase in blood, ascites, or cancer tissues of patients with several cancers (32–35); the $CD4^+CD25^+$ T cells from these organs had also suppressive activities against the immune responses. Recent studies, which evaluated T_R as $FOXP3^+$ lymphocytes showed that $FOXP3^+$ T_R infiltration of the tumor is a significant prognostic factor in the univariate and multivariate analyses in head and neck cancers (43) and Hodgkin's lymphoma (44) and that $CD4^+CD25^+$ T cells contain both $FOXP3^+$ T_R and activated lymphocytes infiltrated in cancer stroma. Our study has shown not only that the prevalence of $FOXP3^+$ T_R is increased in cancer tissue of pancreatic ductal adenocarcinoma but also that this increase is significantly correlated with tumor progression. Furthermore, our study has shown that premalignant lesions of invasive ductal adenocarcinoma of the pancreas, both PanINs and IPMNs, show an increase in the prevalence of T_R during tumor progression. In contrast, infiltration of $CD8^+$ cytotoxic T cells, which were the major lymphocytes to attack neoplastic cells and potential targets for T_R, was prominent in low-grade premalignant lesions, gradually decreased during progression of the tumor, and eventually almost disappeared in PanIN-3, intraductal spreading of adenocarcinoma, and IPMC (Fig. 4J and K). These findings suggest that tumor evasion from host antitumor immunity begins in these premalignant lesions. The details of immune suppression mechanisms of T_R have not been clearly elucidated yet. Initially, the *in vitro* assays proposed the mechanisms were contact dependent and cytokine independent (15–18). Those *in vivo*, however, are thought to be more complex (19–21). Some reports suggested that cytokines, such as TGF-β, play important roles in the event (19, 45). Several studies supported the hypothesis that T_R can localize and expand together with effector T cells in antigen-draining lymph nodes. Inflamed tissue facilitates specific suppression that is initiated by antigenic stimulation and local recruitment of T_R together with effector lymphocytes (21). Another studies provided the findings that tumor antigen-specific T_R at tumor sites have a profound effect on the suppression of antitumor immune responses (31, 46). There is opposite correlation between the prevalence of T_R and the numbers of $CD8^+$ IEL in premalignant lesions during the pancreatic cancer progression, although no interaction of both cells in epithelial layer was observed. It is consistent with the hypothesis that T_R suppress the $CD8^+$ IEL. It also gives rise to the question where T_R affect $CD8^+$ lymphocytes becoming IEL and whether T_R inhibit the recruitment of $CD8^+$ lymphocytes becoming IEL into epithelial layer of pancreatic ducts, although it is possible that neoplastic cells inhibit the recruitment of cytotoxic T cells independent of T_R function. In the future, we need to make clear how these events happen.

The immune surveillance theory of cancer was proposed in the 1970s but remained controversial for a long period. In the last decade, studies with several gene-disrupted or antibody-treated immunocompromised mouse models have provided evidence that the host immune system controls tumor development (3). Nevertheless, the histologic features of cancer immune surveillance in human tissues remain unclear. If the immune surveillance theory applies to pancreatic carcinogenesis, cytotoxic lymphocytes would attack transformed cells or early-stage tumor cells developing in thin or thick pancreatic ducts. Some transformed cells would disappear, whereas others would be resistant to attack and would remain or progress to higher-grade premalignant cells. Our histologic findings may show the process of immune surveillance in the premalignant lesions of pancreatic ductal adenocarcinoma as well as tumor evasion from the host immune system by immunosuppression mediated by $FOXP3^+CD4^+$ T_R.

Our study showed that the high prevalence of T_R in cancer stroma of pancreatic ductal adenocarcinoma was closely correlated with several malignant features, such as distant metastasis, high tumor grade, and advanced pathologic tumor-node-metastasis stage, suggesting that the prevalence of T_R can be a positive indicator of tumor aggressiveness. Several prognostic factors were examined to determine their effect on survival in patients who underwent resection. In

our retrospective study using multivariate analysis for the clinicopathologic variables, lymph node metastasis, distant metastasis, and tumor margins were independent factors for patient survival as reported previously (8, 9). This study showed that the prevalence of T_R in tissue-infiltrating lymphocytes was significantly and negatively correlated with patient survival, independent of tumor-node-metastasis classification, tumor grade, and tumor margins. These findings indicate that the prevalence of T_R is a good predictor of prognosis for patients with ductal adenocarcinoma of the pancreas.

It has been controversial whether the prevalence of T_R in tumor-draining lymph nodes is increased or decreased compared with that in non–tumor-draining lymph nodes (33, 35). Those studies considered $CD4^+CD25^+$ T cells as T_R. In our study, the prevalence of T_R in draining lymph nodes was similar among patients with pancreatic adenocarcinoma, IPMNs, and nonneoplastic lesions. Recently, Chen et al. (19) reported that T_R expand in draining lymph nodes after cognate T-cell receptor stimulation as do naive T cells. More recently, Hiura et al. (47) showed that both T_R and antitumor effector T cells are primed in the same draining lymph nodes of mice with transplanted tumors. They also showed that the $CD4^+CD25^+$ T cells in the draining lymph nodes could be divided into two different populations, $CD62L^{high}CD4^+CD25^+$ T cells that show T_R activity and express Foxp3 and $CD62L^{low}CD4^+CD25^+$ T cells that are effector T cells without T_R activity and Foxp3 expression (47). These findings in murine models imply that T_R in tumor-draining lymph nodes should be expanded, although the prevalence of T_R in $CD4^+$ T cells might be determined by the total spectrum of immune response in the tissues from which the draining lymph nodes collect lymph.

In conclusion, our data suggest that T_R play a role in controlling the immune response to pancreatic ductal carcinoma from the premalignant stage to established cancer. In premalignant lesions, both PanINs and IPMNs, host immune surveillance is prominent in the earlier stages but decreases during tumor progression, inversely correlating with the increase in the prevalence of T_R. A high prevalence of T_R seems to be a marker of poor prognosis.

Acknowledgments

We thank Drs. Yae Kanai, Yuri A. Fukasawa, Hidenori Ojima, and Yoshinori Ino for useful discussions.

References

1. Pardoll D. Does the immune system see tumors as foreign or self? Annu Rev Immunol 2003;21:807–39.
2. Mapara MY, Sykes M. Tolerance and cancer: mechanism of tumor evasion and strategies for breaking tolerance. J Clin Oncol 2004;22:1136–51.
3. Dunn GP, Bruce AT, Ikeda H, Old LJ, Schreiber RD. Cancer immunoediting: from immunosurveillance to tumor escape. Nat Immunol 2002;3:991–8.
4. Jemal A, Murray T, Ward E, et al. Cancer Statistics, 2005. CA Cancer J Clin 2005;55:10–30.
5. Kakizoe T, Yamaguchi N, Mitsuhashi F. Cancer statistics in Japan: foundation for promotion of cancer research 2000. Tokyo, Japan; 2001 p. 3–39.
6. Warshaw AL, Fernandez-del Castillo C. Pancreatic carcinoma. N Engl J Med 1992;326:455–65.
7. Conlon KC, Klimstra DS, Brennan MF. Long-term survival after curative resection for pancreatic ductal adenocarcinoma: clinicopathological analysis of 5-year survivors. Ann Surg 1996;223:273–9.
8. Geer RJ, Brennan MF. Prognostic indicators for survival after resection of pancreatic adenocarcinoma. Am J Surg 1993;165:68–73.
9. Sperti C, Pasquali C, Piccoli A, Pedrazzoli S. Survival after resection for ductal adenocarcinoma of the pancreas. Br J Surg 1996;83:625–31.
10. Hruban RH, Takaori K, Klimstra DS, et al. An illustrated consensus on the classification of pancreatic intraepithelial neoplasia and intraductal papillary mucinous neoplasms. Am J Surg Pathol 2004;28:977–87.
11. Hruban RH, Goggins M, Parsons J, Kern SE. Progression model for pancreatic cancer. Clin Cancer Res 2000;6:2969–72.
12. Biankin AV, Kench JG, Dijkman FP, Biankin SA, Henshall SM. Molecular pathogenesis of precursor lesions of pancreatic ductal adenocarcinoma. Pathology 2003;35:14–24.
13. Longnecker DS, Adler G, Hruban RH, Kloppel G. Intraductal papillary-mucinous neoplasms of the pancreas. In: Hamilton SR, Aaltonen LA, editors. Pathology and genetics. Tumours of the digestive system. WHO classification of tumours. Lyon: IARC Press; 2000. p. 237–40.
14. Cho KR, Vogelstein B. Genetic alterations in the adenoma-carcinoma sequence. Cancer 1992;70:1727–31.
15. Sakaguchi S, Sakaguchi N, Asano M, Itoh M, Toda M. Immunologic self-tolerance maintained by activated T cells expressing IL-2 receptor α-chains (CD25): breakdown of a single mechanism of self-tolerance causes various autoimmune diseases. J Immunol 1995;155:1151–64.
16. Sakaguchi S. Regulatory T cells: key controllers of immunologic self-tolerance. Cell 2000;101:455–8.
17. Dieckmann D, Plottner H, Berchtold S, Berger T, Schuler G. *Ex vivo* isolation and characterization of $CD4^+CD25^+$ T cells with regulatory properties from human blood. J Exp Med 2001;193:1303–10.
18. Shevach EM. $CD4^+CD25^+$ suppressor T cells: more questions than answers. Nat Rev Immunol 2002;2:389–400.
19. Chen ML, Pittet MJ, Gorelik L, et al. Regulatory T cells suppress tumor-specific CD8 T cell cytotoxicity through TGF-β signals *in vivo*. Proc Natl Acad Sci U S A 2005;102:419–24.
20. Sakaguchi S. Naturally arising Foxp3-expressing $CD25^+CD4^+$ regulatory T cells in immunological tolerance to self and non-self. Nat Immunol 2005;6:345–52.
21. von Boehmer H. Mechanisms of suppression by suppressor T cells. Nat Immunol 2005;6:338–44.
22. Brunkow ME, Jeffery EW, Hjerrild KA, et al. Disruption of a new forkhead/winged-helix protein, scurfin, results in the fatal lymphoproliferative disorder of the scurfy mouse. Nat Genet 2001;27:68–73.
23. Chatila TA, Blaeser F, Ho N, et al. *JM2*, encoding a fork head-related protein, is mutated in X-linked autoimmunity-allergic disregulation syndrome. J Clin Invest 2000;106:R75–81.
24. Fontenot JD, Gavin MA, Rudensky AY. Foxp3 programs the development and function of $CD4^+CD25^+$ regulatory T cells. Nat Immunol 2003;4:330–6.
25. Khattri R, Cox T, Yasayko SA, Ramsdell F. An essential role for Scurfin in $CD4^+CD25^+$ T regulatory cells. Nat Immunol 2003;4:337–42.
26. Hori S, Nomura T, Sakaguchi S. Control of regulatory T cell development by the transcription factor Foxp3. Science 2003;299:1057–61.
27. Fontenot JD, Rudensky AY. A well adapted regulatory contrivance: regulatory T cell development and the forkhead family transcription factor Foxp3. Nat Immunol 2005;6:331–7.
28. Fontenot JD, Rasmussen JP, Williams LM, Dooley JL, Farr AG, Rudensky AY. Regulatory T cell lineage specification by the forkhead transcription factor Foxp3. Immunity 2005;22:329–41.
29. Shimizu JS, Yamazaki S, Sakaguchi S. Induction of tumor immunity by removing $CD25^+CD4^+$ T cells: a common basis between tumor immunity and autoimmunity. J Immunol 1999;163:5211–8.
30. Onizuka SI, Tawara J, Shimizu J, Sakaguchi S, Fujita T, Nakayama E. Tumor rejection by *in vivo* administration of anti-CD25 (interleukin-2 receptor α) monoclonal antibody. Cancer Res 1999;59:3128–33.
31. Nishikawa H, Kato T, Tawara I, et al. Accelerated chemically induced tumor development mediated by $CD4^+CD25^+$ regulatory T cells in wild-type hosts. Proc Natl Acad Sci U S A 2005;102:9253–7.
32. Woo EY, Chu CS, Goletz TJ, et al. Regulatory $CD4^+CD25^+$ T cells in tumors from patients with early-stage non-small lung cancer and late-stage ovarian cancer. Cancer Res 2001;61:4766–72.
33. Liyanage UK, Moore TT, Joo HG, et al. Prevalence of regulatory T cells is increased in peripheral blood and tumor microenvironment of patients with pancreas or breast adenocarcinoma. J Immunol 2002;169:2756–61.
34. Ichihara F, Kono K, Takahashi A, Kawaida H, Sugai H, Fujii H. Increased populations of regulatory T cells in peripheral blood and tumor-infiltrating lymphocytes in patients with gastric and esophageal cancers. Clin Cancer Res 2003;9:4404–8.
35. Curiel TJ, Coukos G, Zou L, et al. Specific recruitment of regulatory T cells in ovarian carcinoma fosters immune privilege and predicts reduced survival. Nat Med 2004;10:942–9.
36. Kloppel G, Hruban RH, Longnecker DS, Adler G, Kern SE, Partanen TJ. Ductal adenocarcinoma of the pancreas. In: Hamilton SR, Aaltonen LA, editors. Pathology and genetics. Tumours of the digestive system. WHO classification of tumours. Lyon: IARC Press; 2000. p. 220–30.
37. Hermanek P, Hutter RVP, Sobin LH, Wagner G, Wittekind Ch. TNM Atlas, 4th ed. Berlin: Springer-Verlag; 1997. p. 144–53.
38. Japan Pancreas Society. Classification of pancreatic carcinoma (English Edition). Tokyo: Kanehara; 1998. p. 39.
39. Hiraoka N, Yamada T, Abe H, Hata J. Establishment of three monoclonal antibodies specific for

prespermatogonia and intratubular malignant germ cells in humans. Lab Invest 1997;76:427–38.

40. Hiraoka N, Petryniak B, Nakayama J, et al. A novel, high endothelial venule-specific sulfotransferase expresses 6-sulfo sialyl Lewis(x), an L-selectin ligand displayed by CD34. Immunity 1999;11:79–89.

41. Takahashi Y, Hiraoka N, Onozato K, et al. Solid-pseudopapillary neoplasms of the pancreas in men and women: do they differ? Virchows Arch 2006; 448:561–9.

42. Zelenay S, Lopes-Carvalho T, Caramalho I, Moraes-Fontes MF, Rebelo M, Demengeot J. Foxp3$^+$CD25$^-$ CD4 T cells constitute a reservoir of committed regulatory cells that regain CD25 expression upon homeostatic expansion. Proc Natl Acad Sci U S A 2005;102: 4091–6.

43. Badoual C, Hans S, Rodriguez J, et al. Prognostic value of tumor-infiltrating CD4$^+$ T-cell subpopulations in head and neck cancers. Clin Cancer Res 2006;12: 465–72.

44. Alvaro T, Lejune M, Salvado MT, et al. Outcome in Hodgkin's lymphoma can be predicted from the presence of accompanying cytotoxic and regulatory T cells. Clin Cancer Res 2005;11:1467–73.

45. Nakamura K, Kitani A, Fuss I, et al. TGF-β1 plays an important role in the mechanism of CD4$^+$CD25$^+$ regulatory T cell activity in both humans and mice. J Immunol 2004;174:834–42.

46. Wang HY, Lee DA, Peng G, et al. Tumor-specific human CD4$^+$ regulatory T cells and their ligands: implications for immunotherapy. Immunity 2004;20: 107–18.

47. Hiura T, Kagamu H, Miura S, et al. Both regulatory T cells and antitumor effector T cells are primed in the same draining lymph nodes during tumor progression. J Immunol 2005;175:5058–66.